Punjab University Journal of Mathematics (2024), 56(12), 781-798
https://doi.org/10.52280/pujm.2024.56(12)01

Study of ternary nanoparticles in Oldroyd-B fluid using ethylene glycol

Muhammad Haris Butt
Department of Mathematics, University of Management and Technology, Lahore, Pakistan

*Muhammad Imran Asjad
Department of Mathematics, University of Management and Technology, Lahore, Pakistan
Center for Theoretical Physics, Khazar University, 41 Mehseti str., Baku, AZ1096, Azerbaijan

Muhammad Armaghan Sadiq
Department of Mathematics, University of Management and Technology, Lahore, Pakistan

Abid Hussanan
Department of Mathematics, University of Education, Dera Ghazi Khan, Pakistan

*Corresponding Author
imran.asjad@umt.edu.pk

Received: 16 October, 2023 / Accepted: 09 April, 2025 / Published online: 11 August, 2025

Abstract. This paper presents the expansion of an analytical model for the performance of Oldroyd-B nanofluid, where ethylene glycol is assumed as the base fluid and copper (Cu) tri-nanoparticles are introduced for nanofluid preparation. A systematic strategy is established by converting the related nonlinear governing equations into dimensionless form. To find analytical solutions for the research problem, the Laplace transformation is used as a key tool. This research includes a review of the effects of important variables on the temperature and velocity patterns inside the fluid. In particular, for greater values of the volume fraction of nanoparticles, the temperature is enhanced while a decline in velocity is observed. For comparison is done by choosing different base fluids like kerosene and ethylene glycol and velocities are tested at various temperatures and velocities. The profile can be enhanced for kerosene. Comparative analysis is done by comparing the obtained results to those produced by the mathematical software Mathcad.

AMS (MOS) Subject Classification Codes: 76A05; 76D05; 76T20
Key Words: Oldroyd-B nanofluid; Analytical solutions; Thermal radiation; Magnetic field; Laplace transformation.

1. Introduction

Many researchers are interested in non-Newtonian fluids in the current scientific and technological era since they have more uses than Newtonian fluids. Because shear rate and shear stress are not directly proportional in non-Newtonian fluids, reliable estimation of all relevant characteristics for such fluids is not plausible using a particular model [2, 3, 15]. The traditional Navier equation provides a comprehensive description of these fluids rheological properties and dynamics, including yield stress, memory effects, changes in stress, retardation, relaxation, elongation, and a variety of other phenomena. It is advised

to use a few different models to incorporate the additional nonlinear factors and to assume certain properties. The non-Newtonian behavior of fluids is explained by several concrete models in [4, 18]. There are numerous non-Newtonian fluids found in nutrients such as yogurt, oil, butter, cheese, and soup that serve as examples of the elastic feature. The Oldroyd-B model, which may build flow history and reveal the causes of retardation and relaxation, is an additional suitable and agreeable model to demonstrate the fluid's viscous and elastic characteristics. When the solvent viscosity is zero, the Oldroyd-B model is a restricted example of the Maxwell model [21, 45]. Using a fractional technique and the addition of various nanoparticles [7] were able to solve the Maxwell nanofluid problem. [8] evaluate the nanofluid model using the fractional technique. Analysis of the MHD Oldroyd-B fluid model over a fluctuating vertical belt was successful [16]. Investigated the Oldroyd-B fluid destructive non-linear flow caused by stretchy sheets using the HPM method [44]. Analytical fractional Oldroyd-B model through shifting channel explained by [27]. OHAM was used to evaluate the Oldroyd-B model's nano-material stagnation point flow [20].

In 1995, to introduced nanofluid for the first time, bringing about a progressive transformation in thermal transportation and resolving the entropy issue in temperature management systems [12]. Nano-sized pieces of metallic elements, oxides, or carbides, ranging in size from 1 nm to 100 nm, are combined with base fluids like ethylene glycol, carotene, etc, to create nanofluids. Nanoparticles increase the exterior region of thermal conduction and thermal conductivity when supplied to a fluid, which increases the rate of heat transfer. Nanofluids are the ideal coolant for high-temperature transmission systems like electronic cooling, heaters, and heat exchangers. The use of nanofluids based on graphene has improved polymerase chain reaction in a professional manner [40]. In freezing climates, rooms are heated more efficiently with the use of nanofluids. Utilizing nanofluids can help cut costs, energy waste, and pollution. According to [28], nanofluids increase energy conservation by reducing heat exchanger volume. One study by [11] on nanofluid found that the suspended nanoparticles remarkably increase the convective heat transfer coefficient of the base fluid. Worked on the measurements of nanofluid viscosity and its implications for thermal applications. Nanofluids intended for enhanced oil recovery were presented by [29]. Studied the stable colloidal suspensions of kerosene-based magnetite, polyaphaolefin-based alumina spheres and alumina nanorods, and their results revealed that the specific heat capacity of polyalphaolefin-based aluminum oxide nanofluids improves when volume fraction and particle size increase [9].

Due to their ability to transmit heat in their true mode, the significance of nanofluids has received attention on a worldwide scale in recent years. Researched on the use of nanofluids in thermosyphons [31]. With the use of nanofluids, Bretado-de los [34] research focused on solar thermal heat exchangers. The best lubricants are nanofluids, according to have investigated the smooth impacts of nano-particles on the rotating nanofluids flow [8]. The research has a significant influence on this approach [10]. The importance of mathematical models in connecting the various physical phenomena that occur in everyday life is greater. Differential equations with a few beginning and boundary conditions make up these models. These derivatives may be fractional derivatives of non-integer order or integer derivatives of different orders non-integer fractional derivatives, however, come up with a wide application in the innovative, developed world. Since fractional models more closely

approximate the form of physical systems. Additionally, a fractional constraint is a component of the result that helps to manage the flow regime and provides a more succinct explanation of the memory outcome. As a result, fractional models are thought to be superior to conventional models. By using fractional differential equations, it is possible to describe a variety of engineering processes as well as physical systems. Certain models were found to clearly specify these fractional differential equations. The fractional derivative can be used to enhance a variety of natural wonders in thermal transfer, industrial, electrical circuits, bioengineering, and signal processing. By employing fractional derivatives, viscoelastic checking in macromolecules can be effectively illustrated. Investigate the outcomes of heat absorption/generation on the MHD Oldroyd-B fluid across an unrestricted plate placed in a porous surface with ramp wall temperature and velocity [38, 41]. Infinite vertical tubes containing MHD flows of Oldroyd-B fluids subjected to nonlinear thermal radiation are discussed by [5]. In the existence of a tilted external magnetic field, analyzed the analytical solutions of the Oldroyd-B fluid model of such an inclined plate covered in a porous medium, whether stationary or continuously oscillating [42]. Discovered more about the mass and heat transmission of ramped-condition MHD Oldroyd-B fluid. Examined how carbon nanotubes in an Oldroyd-B nanofluid can increase heat transport in incompressible MHD convective flow [6]. By utilizing the Atangana Baleanu fractional derivative via the Laplace transform technique, we examined the temperature and mass transmission of the Oldroyd-B nanofluid [43]. Viscous dissipation refers to the destruction of viscous strains by a changing velocity gradient. As a result of viscous dissolution, which is an irreversible process that causes the fluid to heat up, the fluid's viscosity absorbs energy from its motion and converts it to internal energy. Successful outcomes with the use of viscous dissolution, magnetic, and energy fields on nanofluid are taken into consideration within [35]. The detailed viscous dissipation effect was first found [19]. The influence of viscous dissipation on entropy was analyzed [17]. Entropy is essentially a measure of a system's disorder or randomness. Using a magnetic field [32] evaluated the 2D flow of a Carreau-ternary hybrid nanoliquid over the permeable stretching sheet. The viscoelastic fluid flow caused by a linearly extending surface is examined in [7, 22] research to determine the impacts of porous and viscous dissipation on entropy formation.

To examined a continuous, incompressible, and 2D flow of a viscous ternary nanofluid composed of sodiumalginate, and containing copper and alumina nanoparticles close to a stretchy curved surface [13]. Investigated a 3D MHD ternary hybrid nano liquid flow inside porous materials in the region of a stretched surface for its heat and mass transport properties [33]. Investigate the effects of particle and heat accumulations of a water-based ternary hybrid $Al_2O_3 - CuO - TiO_2$ nanofluid on the dynamic viscosity [36]. In a second-grade scenario across an infinite vertical plate, investigated the results of the Atangana-Baleanu (AB) time-fractional integral on a fluid comprising a ternary nanoparticle suspension [37]. Examined the mass and heat transmission in MHD ternary ethylene-glycol-based hybrid nanofluid above a revolving 3D exterior with the influence of suction velocity [30]. To present a narrative theoretical framework for ternary nanoparticles to enhance heat transmission [1, 26]. To observe the behavior of a ternary nanofluid on a slippery exterior. After the narrative previously addressed, it is important to notice that the MHD Oldroyd-B nanofluid model numerical solution, without taking into consideration thermal radiation, variable viscosity, or a heat source/sink, uses the Laplace transformation [24, 39].

While previous studies have explored various types of nanoparticles and fluid configurations in Newtonian and non-Newtonian systems, limited attention has been given to incorporating such models particularly in the context of ternary nanofluids. This study addresses this gap by the Oldroyd-B nanofluid model subjected to a magnetic field and incorporating heat source/sink and thermal radiation effects. The novelty of this work lies in applying the Laplace transform technique to derive exact analytical solutions for temperature and velocity profiles, which are then compared to existing models. The results demonstrate that the inclusion of ternary nanoparticles significantly enhances thermal conductivity and flow behavior, offering a more robust and efficient framework for heat transfer applications. This contribution advances the modeling of non-Newtonian nanofluids by combining fractional dynamics with multi-nanoparticle synergy.

2. Mathematical Formulation

Figure 1 depicts the flow dynamics geometry of an incompressible Oldroyd-B nanofluid adjacent to a vertical plate. The plate is positioned along the y-axis, with the x-axis extending perpendicularly outward from the plate surface. Initially (at t ≤ 0), both the fluid and the plate are at rest and maintained at a uniform temperature, θ_∞. For times $t > 0$, the plate begins to vertically $(U_0 H_{ct})$, and its temperature is increased to θ_ω. This temperature difference drives an unstable natural convection flow, resulting in upward fluid motion parallel to the plate (in the positive y-direction). A uniform magnetic field, denoted as B_0, is applied perpendicular to the plate, acting along the positive x-axis. The figure illustrates the development of momentum and thermal boundary layers adjacent to the plate, influenced by the presence of nanoparticles dispersed within the Oldroyd-B base fluid. The velocity profile is assumed to have the form $V(u(y,t),0,0)$, indicating that the flow is primarily in the x direction.

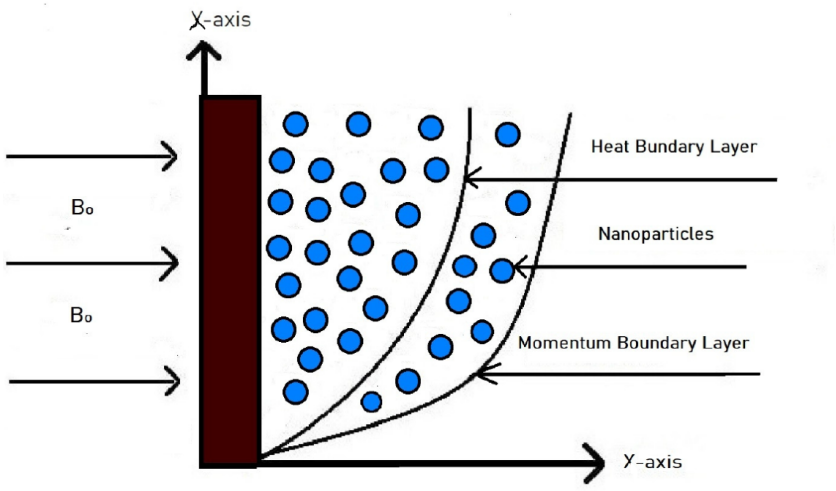

FIGURE 1. The flow dynamics geometry.

The Oldroyd-B fluid constitutive flow equations are provided in [46] as,

$$\boldsymbol{V}.\nabla = 0, \quad \rho\left[(\boldsymbol{V}.\nabla)\,\boldsymbol{V} + \frac{\partial \boldsymbol{V}}{\partial t}\right] = div(\boldsymbol{T}) + \rho bg + \mathrm{M} \times \boldsymbol{J}, \tag{2. 1}$$

$$\begin{aligned}\rho_{mnf}\left(1+\lambda_1\frac{\partial}{\partial t}\right)\left(\frac{\partial u}{\partial t}\right) = (1+\lambda_2\frac{\partial}{\partial t})\mu_{mnf}\frac{\partial^2 u}{\partial y^2} \\ + g(\rho\beta_\theta)_{mnf}\left(1+\lambda_1\frac{\partial}{\partial t}\right)(\theta-\theta_\infty) \\ - \left(1+\lambda_1\frac{\partial}{\partial t}\right)\sigma_{mnf}B_o^2 u.\end{aligned} \tag{2. 2}$$

According to [47], the energy equation for a heat source/sink with thermal radiations effect,

$$(\rho C_p)_{mnf}\left(\frac{\partial \theta}{\partial t}\right) = K_{mnf}\frac{\partial^2\theta}{\partial y^2} - \frac{\partial q_r}{\partial y} + Q(\theta-\theta_\infty), \tag{2. 3}$$

where, $\rho C_p)_{mnf}$, represents the effective heat capacity of the nanofluid. This correction ensures physical consistency and aligns the equation with the governing principles of energy conservation in fluid dynamics. The q_r under the Rosseland estimation in [48] is,

$$q_r = \left(\frac{-4\sigma^*}{3k^*}\right)\frac{\partial\theta^4}{\partial y}, \tag{2. 4}$$

where, k^* is the absorption constant, σ^* is Stefan Boltzmann constant, Extending θ^4 about θ_∞ utilising the Taylor series,

$$\theta^4 = 4\theta_\infty^3\theta^{'} - \theta_\infty^4. \tag{2. 5}$$

By neglecting the elevated power of θ and utilising equations (10-11) in equation (9), also multiply with $(1+\lambda_2\frac{\partial}{\partial t})$. Equation (9) assumes the following shape. The operator $(1+\lambda_2\frac{\partial}{\partial t})$ is used to model the relaxation effects in the heat flux as per the Cattaneo-Christov heat flux theory. This theory accounts for thermal relaxation time λ_2 which is significant in cases where transient effects in heat conduction cannot be ignored. By applying this operator, the model captures the time-dependent behavior of thermal relaxation, which is essential for accurately describing heat transfer in nanofluids with thermal memory effects.

$$\begin{aligned}(\rho C_p)_{mnf}\left(1+\lambda_2\frac{\partial}{\partial t}\right)\left(\frac{\partial\theta}{\partial t}\right) = K_{mnf}\left(1+\lambda_2\frac{\partial}{\partial t}\right)\frac{\partial^2\theta}{\partial y^2} \\ + \frac{16\sigma^*\theta_\infty^3}{3k^*}\frac{\partial\theta}{\partial t} + \left(1+\lambda_2\frac{\partial}{\partial t}\right)Q(\theta-\theta_\infty).\end{aligned} \tag{2. 6}$$

In [49] identical initial and boundary conditions are,

$$u(y,0)=0,\ \ u(0,t)=u_0H(t),\ \ u(\infty,t)=0, \tag{2. 7}$$

$$\theta(y,0)=\theta_\infty,\ \ \theta(0,t)=\theta_w,\ \ \theta(\infty,t)=\theta_\infty. \tag{2. 8}$$

The non-dimensional quantities in the suggested model are listed below,

$$u^*=\frac{u}{u_0},\ t^*=\frac{u_0^2}{\nu}t,\ \theta^*=\frac{\theta-\theta_\infty}{\theta_w-\theta_\infty},\ \lambda_1^*=\frac{u_0^2}{\nu}\lambda_1,\ \lambda_2^*=\frac{u_0^2}{\nu}\lambda_2,\ y^*=\frac{u_0y}{\nu},$$

The relations and properties of nanoparticles are as follow,

$$\begin{aligned}&\mathrm{Gr}=\frac{\nu g(\beta_\theta)_f(\theta_w-\theta_\infty)}{u_0^3},\quad H_a^2=M=\frac{\sigma_fB_0^2\nu}{\rho_fu_0^2},\quad \mathrm{Pr}=\frac{\mu(C_p)_f}{K_f},\\&\mathrm{Nr}=\frac{16\sigma^*\theta_\infty^3}{a_5\cdot 3k^*K_f},\quad Q_0=\frac{Q\nu}{a_5K_fu_0^2}.\end{aligned} \tag{2. 9}$$

The relation for nanofluids are inclined in [48] as,

$$\begin{aligned}\frac{\rho_{mnf}}{\rho_f}=a_1&=\left[(1-(\phi_1+\phi_2+\phi_3))+\phi_1\frac{\rho_{S1}}{\rho_f}+\phi_2\frac{\rho_{S2}}{\rho_f}+\phi_3\frac{\rho_{S3}}{\rho_f}\right],\\\frac{(\rho\beta_\theta)_{mnf}}{(\rho\beta_\theta)_f}=a_2&=\left[(1-(\phi_1+\phi_2+\phi_3))+\phi_1\frac{(\rho\beta_\theta)_{S1}}{(\rho\beta_\theta)_f}+\phi_2\frac{(\rho\beta_\theta)_{S2}}{(\rho\beta_\theta)_f}+\phi_3\frac{(\rho\beta_\theta)_{S3}}{(\rho\beta_\theta)_f}\right],\\\frac{\mu_{mnf}}{\mu_f}=a_3&=[\frac{1}{(1-(\phi_1+\phi_2+\phi_3))^{2.5}}],\\\frac{(\rho C_p)_{mnf}}{(\rho C_p)_f}=a_4&=\left[(1-(\phi_1+\phi_2+\phi_3))+\phi_1\frac{(\rho C_p)_{S1}}{(\rho C_p)_f}+\phi_2\frac{(\rho C_p)_{S2}}{(\rho C_p)_f}+\phi_3\frac{(\rho C_p)_{S3}}{(\rho C_p)_f}\right],\end{aligned} \tag{2. 10}$$

$$\frac{k_{mnf}}{k_f}=a_5=\left[\begin{array}{l}\phi_1k_1+\phi_2k_2+\phi_3k_3+2(\phi_1+\phi_2+\phi_3)k_f\\+2(\phi_1+\phi_2+\phi_3)(\phi_1k_1+\phi_2k_2+\phi_3k_3)\\-2(\phi_1+\phi_2+\phi_3)^2k_f\\\hline\phi_1k_1+\phi_2k_2+\phi_3k_3+2(\phi_1+\phi_2+\phi_3)k_f\\-(\phi_1+\phi_2+\phi_3)(\phi_1k_1+\phi_2k_2+\phi_3k_3)\\+(\phi_1+\phi_2+\phi_3)^2k_f\end{array}\right] \tag{2. 11}$$

$$\frac{(\sigma)_{mnf}}{(\sigma_f)_f}=a_6=\left[1+\frac{3(\frac{\sigma_s}{\sigma_f}-1)\phi}{(\frac{\sigma_s}{\sigma_f}-2)-(\frac{\sigma_s}{\sigma_f}-1)\phi}\right],$$

$$b_1 = \frac{a_3}{a_1},\ b_2 = \frac{a_2}{a_1},\ b_3 = \frac{a_6}{a_1},\ b_4 = \frac{a_4}{a_5},\ b_5 = \frac{a_3}{a_5},\ b_6 = \frac{a_6}{a_5}. \tag{2. 12}$$

We have below equations by using equation (15)-(17) in equationas (8,12-14),

$$(1+\lambda_1\frac{\partial}{\partial t})\left(\frac{\partial u}{\partial t}\right) = (1+\lambda_2\frac{\partial}{\partial t})b_1\frac{\partial^2 u}{\partial y^2} + b_2 G_r(1+\lambda_1\frac{\partial}{\partial t})\theta - b_3 H_a^2(1+\lambda_1\frac{\partial}{\partial t})u, \tag{2. 13}$$

Equation (19) is based on the Cattaneo-Christov heat flux model, which extends Fourier's law by incorporating a relaxation time parameter (λ_2) to account for thermal memory effects. This model is particularly suitable for describing heat transfer in systems with high thermal gradients or time-dependent effects, such as nanofluids. The presence of the operator $(1 + \lambda_2\frac{\partial}{\partial t})$ ensures that the model captures the transient behavior of heat conduction with relaxation effects. The parameter Pr represents the Prandtl number, which characterizes the relative importance of momentum diffusivity (viscosity) to thermal diffusivity. The parameter Nr denotes the thermal radiation effect, while Q_0 represents the heat generation or absorption coefficient. These terms collectively form a comprehensive model for analyzing heat transfer in nanofluid systems with complex interactions.

$$b_4\,\mathrm{Pr}(1+\lambda_2\frac{\partial}{\partial t})\left(\frac{\partial \theta}{\partial t}\right) = (1+\mathrm{Nr})(1+\lambda_2\frac{\partial}{\partial t})\frac{\partial^2\theta}{\partial y^2} + (1+\lambda_2\frac{\partial}{\partial t})Q_0\theta. \tag{2. 14}$$

The first term is represents the time-dependent heat diffusion equation, incorporating the Prandtl number and thermal relaxation effects. Second accounts for the combined effects of thermal radiation and relaxation in heat conduction. Third represents heat generation or absorption with thermal memory effects. with initial and boundary conditions,

$$u(y,0) = 0,\ \ u(0,t) = H(t),\ \ u(\infty,t) = 0, \tag{2. 15}$$

$$\theta(y,0) = 0,\ \ \theta(0,t) = 1,\ \ \theta(\infty,t) = 0. \tag{2. 16}$$

2.1. **Heat Equation.** Laplace transform applied to the equation (19), we have

$$b_4\,\mathrm{Pr}(1+\lambda_2 s)s\bar{\theta} = (1+\mathrm{Nr})(1+\lambda_2 s)\frac{\partial^2\bar{\theta}}{\partial y^2} + (1+\lambda_2 s)Q_0\bar{\theta}, \tag{2. 17}$$

Apply Laplace on equation (21),

$$\bar{\theta}(y,0) = 0, \quad \bar{\theta}(0,s) = \frac{1}{s}, \quad \bar{\theta}(\infty,s) = 0. \tag{2. 18}$$

Using equation (23) in equation (22), the general solution of heat equation becomes ,

$$\bar{\theta}(y,s) = \frac{1}{s}e^{-y\sqrt{\frac{b_4 Prs - Q_0}{1+\mathrm{Nr}}}}, \tag{2. 19}$$

Finding the inverse formula for equation (24) is challenging since the exponential form is so intricate. To determine the inverse analytically, we utilized the exponential function series form for more appropriate expression. Hence,

$$\bar{\theta}(y,s)=\frac{1}{s}+\sum_{a_1=1}^{\infty}\sum_{b_1=1}^{\infty}\frac{(-y)^{a_1}\ (Pr)^{\frac{a_1}{2}-b_1}(-Q_0)^{b_1}\ (b_4)^{\frac{a_1}{2}-b_1}\ \Gamma(\frac{a_1}{2}+1)}{a_1!\ b_1!\ s^{1+b_1-\frac{a_1}{2}}\ (1+\mathrm{Nr})^{\frac{a_1}{2}}\ \Gamma(\frac{a_1}{2}+1-b_1)}, \tag{2. 20}$$

We get the equation (26) by taking inverse Laplace of equation (25),

$$\theta(y,t)=1+\sum_{a_1=1}^{\infty}\sum_{b_1=1}^{\infty}\frac{(-y)^{a_1}\ (Pr)^{\frac{a_1}{2}-b_1}(-Q_0)^{b_1}\ t^{b_1-\frac{a_1}{2}}\ (b_4)^{\frac{a_1}{2}-b_1}\ \Gamma(\frac{a_1}{2}+1)}{a_1!\ b_1!\ (1+\mathrm{Nr})^{\frac{a_1}{2}}\ \Gamma(\frac{a_1}{2}+1-b_1)\,\Gamma(1+b_1-\frac{a_1}{2})}. \tag{2. 21}$$

2.2. **Momentum Equation.** Laplace transform is applied to the equations (18) and (20), respectively

$$(1+\lambda_1 s)s\bar{u}=(1+\lambda_2 s)b_1\frac{\partial^2\bar{u}}{\partial y^2}+b_2\mathrm{Gr}(1+\lambda_1 s)\bar{\theta}-b_3Ha^2(1+\bar{\lambda_1}s)\bar{u}, \tag{2. 22}$$

$$\bar{u}(y,0)=0,\quad \bar{u}(0,s)=1,\quad \bar{u}(\infty,s)=0, \tag{2. 23}$$

The general solution of equation (27) subjected to equation (28),

$$\begin{aligned}\bar{u}(y,s)&=-\frac{b_2\,\mathrm{Gr}\,(1+\lambda_1 s)}{b_1 s(1+\lambda_2 s)}\cdot\frac{e^{-y\sqrt{\dfrac{b_4\,\mathrm{Pr}\,s-Q_0}{1+\mathrm{Nr}}}}}{\left[D^2-\dfrac{(1+\lambda_1 s)}{(1+\lambda_2 s)}\cdot\left(\dfrac{s+b_3H_a^2}{b_1}\right)\right]}\\&=-\frac{b_2\,\mathrm{Gr}\,(1+\lambda_1 s)}{b_1 s(1+\lambda_2 s)}\cdot\frac{e^{-y\sqrt{\dfrac{b_4\,\mathrm{Pr}\,s-Q_0}{1+\mathrm{Nr}}}}}{\left[\dfrac{b_4\,\mathrm{Pr}\,s-Q_0}{1+\mathrm{Nr}}-\dfrac{(1+\lambda_1 s)}{(1+\lambda_2 s)}\cdot\left(\dfrac{s+b_3H_a^2}{b_1}\right)\right]}\end{aligned}$$

Hence

$$\bar{u}=\frac{1}{s}e^{-y\sqrt{\frac{[1+\lambda_1 s]}{[1+\lambda_2 s]}(\frac{s+b_3Ha^2}{b_1})}}+\frac{b_2\mathrm{Gr}(1+\lambda_1 s)}{b_1 s(1+\lambda_2 s)}\frac{e^{-y\sqrt{\frac{[1+\lambda_1 s]}{[1+\lambda_2 s]}(\frac{s+b_3Ha^2}{b_1})}}}{[\frac{b_4Prs-Q_0}{1+\mathrm{Nr}}-\frac{[1+\lambda_1 s]}{[1+\lambda_2 s]}(\frac{s+b_3H_a^2}{b_1})]}$$

$$-\frac{b_2\mathrm{Gr}(1+\lambda_1 s)}{b_1 s(1+\lambda_2 s)}\frac{e^{-y\sqrt{\frac{b_4Prs-Q_0}{1+\mathrm{Nr}}}}}{[\frac{b_4Prs-Q_0}{1+\mathrm{Nr}}-\frac{[1+\lambda_1 s]}{[1+\lambda_2 s]}(\frac{s+b_3H_a^2}{b_1})]}.$$

Finding the inverse formula for the above equation is challenging since the exponential form is so intricate. To determine the inverse analytically, we utilized the exponential

function series form for a more appropriate expression.

$$\bar{u}(y,s) = \frac{1}{s} + \sum_{a_2=0}^{\infty}\sum_{b_2=0}^{\infty}\sum_{c_2=0}^{\infty}\sum_{d_2=0}^{\infty} \frac{(-y)^{a_2}(b_3)^{\frac{a_2}{2}-d_2}(Ha^2)^{\frac{a_2}{2}-d_2}(\lambda_1)^{b_2}(-\lambda_2)^{c_2}}{a_2!\,b_2!\,c_2!\,d_2!\,(b_1)^{\frac{a_2}{2}}\,s^{1-b_2-c_2-d_2}}$$
$$\times \frac{\Gamma\left(\frac{a_2}{2}+1\right)^2\Gamma\left(\frac{a_2}{2}+c_2\right)}{\Gamma\left(\frac{a_2}{2}+1-b_2\right)\Gamma\left(\frac{a_2}{2}\right)\Gamma\left(\frac{a_2}{2}+1-d_2\right)}$$
$$+ \sum_{a_3=0}^{\infty}\cdots\sum_{j_3=0}^{\infty} \frac{(-y)^{a_3} b_2\,\mathrm{Gr}\,(-1)^{h_3}(b_3)^{\frac{a_3}{2}+g_3-d_3}(Ha^2)^{\frac{a_3}{2}+g_3-d_3}(\lambda_1)^{i_3+b_3}(-\lambda_2)^{j_3+c_3}}{a_3!\cdots j_3!\,s^{2+e_3+g_3+h_3+i_3+j_3-2f_3-b_3-c_3-d_3}}$$
$$\times \frac{(Q_0)^{e_3+h_3}(1+\mathrm{Nr})^{1-f_3}\Gamma\left(\frac{a_3}{2}+1\right)^2\Gamma\left(\frac{a_3}{2}+c_3\right)\Gamma(f_3+1)}{(b_1)^{1+f_3+\frac{a_3}{2}}(b_4)^{1+e_3+h_3-f_3}(\mathrm{Pr})^{1+e_3+h_3-f_3}}$$
$$\times \frac{\Gamma(2+f_3)\Gamma(1+f_3+j_3)}{\Gamma\left(\frac{a_3}{2}\right)\Gamma\left(\frac{a_3}{2}+1-b_3\right)\Gamma\left(\frac{a_3}{2}+1-d_3\right)\Gamma(1+f_3)\Gamma(f_3+1-g_3)\Gamma(f_3+1-h_3)\Gamma(2+f_3-i_3)}$$
$$- \sum_{a_4=0}^{\infty}\cdots\sum_{h_4=0}^{\infty} \frac{(-y)^{g_4} b_2\,\mathrm{Gr}\,(-1)^{h_4+d_4}(b_3)^{c_4}(Ha^2)^{c_4}(\lambda_1)^{e_4}(-\lambda_2)^{f_4}}{c_4!\cdots h_4!\,s^{2+a_4+c_4+d_4+e_4+h_4+f_4-2b_4-\frac{g_4}{2}}}$$
$$\times \frac{(Q_0)^{a_4+d_4+h_4}(1+\mathrm{Nr})^{1-b_4-\frac{g_4}{2}}\Gamma(b_4+1)^2\Gamma(2+b_4)\Gamma(1+b_4+f_4)\Gamma\left(\frac{g_4}{2}+1\right)}{(b_1)^{1+b_4}(b_4)^{1+a_4+d_4+h_4-b_4-\frac{g_4}{2}}(\mathrm{Pr})^{1+a_4+d_4+h_4-b_4-\frac{g_4}{2}}}$$
$$\times \frac{1}{\Gamma(1+b_4-c_4)\Gamma(1+b_4-d_4)\Gamma(2+b_4-e_4)\Gamma(1+b_4)\Gamma\left(1+\frac{g_4}{2}-h_4\right)}.$$

We get the following equation by taking the inverse Laplace of the above equation,

$$u(y,t) = 1 + \sum_{a_2=0}^{\infty}\sum_{b_2=0}^{\infty}\sum_{c_2=0}^{\infty}\sum_{d_2=0}^{\infty} \frac{(-y)^{a_2}\,(b_3)^{\frac{a_2}{2}-d_2}\,(Ha^2)^{\frac{a_2}{2}-d_2}\,(\lambda_1)^{b_2}\,(-\lambda_2)^{c_2}\,t^{-b_2-c_2-d_2}\,\Gamma\left(\frac{a_2}{2}+1\right)^2\,\Gamma\left(\frac{a_2}{2}+c_2\right)}{a_2!\,b_2!\,c_2!\,d_2!\,(b_1)^{\frac{a_2}{2}}\,\Gamma\left(\frac{a_2}{2}+1-b_2\right)\,\Gamma\left(\frac{a_2}{2}\right)\,\Gamma\left(\frac{a_2}{2}+1-d_2\right)\,\Gamma(1-b_2-c_2-d_2)}$$
$$+ \sum_{a_3=0}^{\infty}\sum_{b_3=0}^{\infty}\sum_{c_3=0}^{\infty}\sum_{d_3=0}^{\infty}\sum_{e_3=0}^{\infty}\sum_{f_3=0}^{\infty}\sum_{g_3=0}^{\infty}\sum_{h_3=0}^{\infty}\sum_{i_3=0}^{\infty}\sum_{j_3=0}^{\infty} \frac{(-y)^{a_3}\,b_2\,\mathrm{Gr}\,(-1)^{h_3}\,(b_3)^{\frac{a_3}{2}+g_3-d_3}\,t^{1+e_3+g_3+h_3+i_3+j_3-2f_3-b_3-c_3-d_3}}{a_3!\,b_3!\,c_3!\,d_3!\,g_3!\,h_3!\,i_3!\,j_3!\,(b_1)^{1+f_3+\frac{a_3}{2}}\,(b_4)^{1+e_3+h_3-f_3}}$$
$$\times \frac{(\lambda_1)^{i_3+b_3}\,(-\lambda_2)^{j_3+c_3}\,(Q_0)^{e_3+h_3}\,(1+\mathrm{Nr})^{1-f_3}\,(b_3)^{\frac{a_3}{2}+g_3-d_3}\,(Ha^2)^{\frac{a_3}{2}+g_3-d_3}\,\Gamma\left(\frac{a_3}{2}+1\right)^2\,\Gamma\left(\frac{a_3}{2}+c_3\right)}{(Pr)^{1+e_3+h_3-f_3}\,\Gamma\left(\frac{a_3}{2}\right)\,\Gamma\left(\frac{a_3}{2}+1-b_3\right)\,\Gamma\left(\frac{a_3}{2}+1-d_3\right)\,\Gamma(1+f_3)}$$
$$\times \frac{\Gamma(f_3+1)\,\Gamma(2+f_3)\,\Gamma(1+f_3+j_3)\,\Gamma(f_3+1)}{\Gamma(f_3+1-g_3)\,\Gamma(f_3+1-h_3)\,\Gamma(2+f_3-i_3)\,\Gamma(2+e_3+g_3+h_3+i_3+j_3-2f_3-b_3-c_3-d_3)}$$
$$- \sum_{a_4=0}^{\infty}\sum_{b_4=0}^{\infty}\sum_{c_4=0}^{\infty}\sum_{d_4=0}^{\infty}\sum_{e_4=0}^{\infty}\sum_{f_4=0}^{\infty}\sum_{g_4=0}^{\infty}\sum_{h_4=0}^{\infty} \frac{(-y)^{g_4}\,b_2\,\mathrm{Gr}\,(-1)^{h_4+d_4}\,(b_3)^{c_4}\,(Ha^2)^{c_4}\,t^{1+a_4+c_4+d_4+e_4+h_4+f_4-2b-\frac{g_4}{2}}}{c_4!\,d_4!\,e_4!\,g_4!\,h_4!\,(b_1)^{1+b_4}\,(b_4)^{1+a_4+d_4+h_4-b_4-\frac{g_4}{2}}}$$
$$\times \frac{(\lambda_1)^{e_4}\,(-\lambda_2)^{f_4}\,(Q_0)^{a_4+d_4+h_4}\,(1+\mathrm{Nr})^{1-b_4-\frac{g_4}{2}}\,\Gamma(b_4+1)^2}{(Pr)^{1+a_4+d_4+h_4-b_4-\frac{g_4}{2}}\,\Gamma(1+b_4-c_4)\,\Gamma(1+b_4-d_4)\,\Gamma(2+b_4-e_4)}$$
$$\times \frac{\Gamma(2+b_4)\,\Gamma(1+b_4+f_4)\,\Gamma\left(\frac{g_4}{2}+1\right)}{\Gamma(1+b)\,\Gamma\left(1+\frac{g_4}{2}-h_4\right)\,\Gamma\left(2+a_4+c_4+d_4+e_4+h_4+f_4-2b-\frac{g_4}{2}\right)}.$$

TABLE 1. Thermodynamic properties of nanaoparticles and the base fluid from [23, 25, **?**]:

Material	$\rho(kgm^{-3})$	$C_p(JKg^{-1}k^{-1})$	k$(Wm^{-1}k^{-1})$	$\beta(k^{-1})$	$\sigma(\Omega m)^{-1}$
Ethylene glycol	1116.6	2383	0.249	65x10^{-5}	1.07x10^{-7}
Copper	8933	385	401	1.67x10^{-5}	5.96x10^{7}
Aluminium	3970	765	40	0.85x10^{-5}	3.69x10^{7}
Silver	10500	235	429	189x10^{-5}	3.6x10^{7}
Keroscene	820	2090	0.145	1.2×10^{-3}	≈ 0

3. GRAPHICAL DISCUSSION AND RESULTS

The key analytical physical and findings interpretation of various evolving constraint, including the magnetic field constraint, Prandtl number, fractional constraint, Eckert number, time relaxation constraint, radiation constraint, Nusselt number, volume fraction, entropy generation constraint, skin friction constraint of nanoparticles, and Bejan number, in this area of the research effort are all summarized. Using Mathcad, the outcomes of the velocity profile $u(y,t)$ and the temperature profile $\theta(y,t)$, as well as the consequences of the identified limitations, are all taken into consideration. The Laplace transform has been used to analytically solve the related and nonlinear model.

Figure 2 was purposefully created to show how the concentration of nanoparticles $0 < \phi_1$, ϕ_2, and $\phi_3 < 0.04$ affects the temperature profile. From rising the concentration of nanoparticles, the rising temperature is noticed. Growing the concentration of nanoparticles causes thermal conductivity to increase, which eventually causes to increase in thickness and temperature too.

Figure 3 shows intentionally how Pr performs in relation to the temperature field. The distribution of temperature decreases when Pr values are magnified. The Pr number is the reciprocal of the momentum-to-heat diffusivity ratio. Because fluids with lower Pr number estimates have better thermal conductivity, temperature leaves the heated surface more quickly and earlier compared to fluids with higher Pr number values. As a result, nanoparticles use two distinct base fluids, such as kerosene and ethylene glycol. Choosing ethylene glycol as the base fluid with trihybrid nanoparticles is a more efficient approach to improving thermal conductivity in comparison to kerosene. Due to high Pr, temperature decreases due to high thermal conductivity.

Figure 4 is suggested as an illustration of the influence of nanoparticle concentration on the velocity field. When the concentration of nanoparticles rises, it is clear that the velocity profile is descending. Physically, due to the enhancement of the concentration of tri-hybrid nanoparticles, viscous forces became stronger, ultimately thickening the boundary layer and reducing the fluid velocity.

Figure 5 illustrates the impact of Pr on the velocity field. Improving Pr values causes the velocity distribution to decrease. This is due to the fact that the heat conductivities of different base fluids differ (kerosene and ethylene glycol). Velocity changed to composite, and a further characteristic peak may be seen close to the plate. As a result, the velocity distribution condenses as the border sheet thickness increases.

Figure 6 displays the impact of the Grashöf number $0 \leq \mathrm{Gr} \leq 0.3$ on the velocity profile. Growing Gr values cause the increase in the velocity of fluid. The Gr number is a proportion between buoyant and viscous forces. The buoyancy forces rise for increased Gr values, increasing the induced flow as a result and enhancing the fluid's velocity.

Figure 7 demonstrates the impact of a magnetic field on fluid velocity. Fluid velocity decreases as the strength of the magnetic field parameter $2 \leq \mathrm{Ha} \leq 6$ increases. That is explicable since increasing the magnetic field strength actually increased the Lorentz force, which exhibits a high barrier to fluid movement.

The outcome of the time relaxation constraint $0 \leq \lambda_1 \leq 0.04$ on the velocity profile is seen in Figure 8. For magnified values of the time relaxation constraint, it is possible to determine that the velocity profile is decreasing.

The outcome of the time relaxation constraint $0 \leq \lambda_2 \leq 0.4$ on the velocity profile is seen in Figure 9. For increased values of the temporal relaxation constraint, it is possible to determine that the velocity profile is expanding.

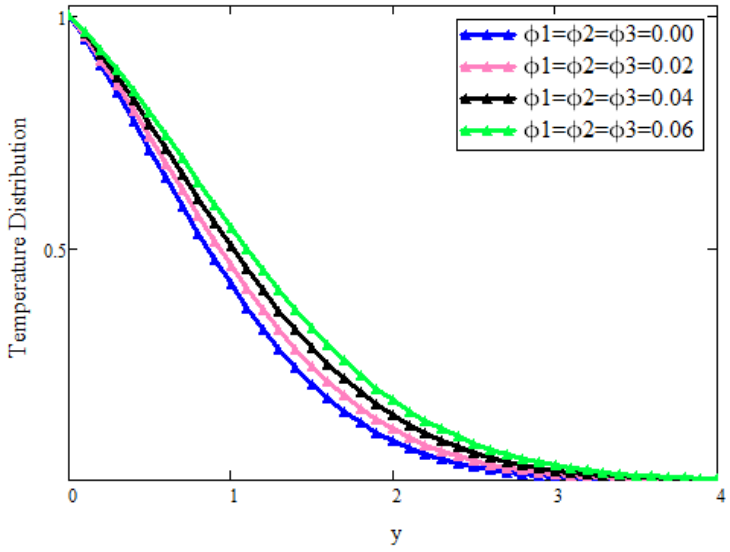

FIGURE 2. The result of temperature distribution on volume fraction parameter of nanofluid ϕ_1,ϕ_2,ϕ_3.

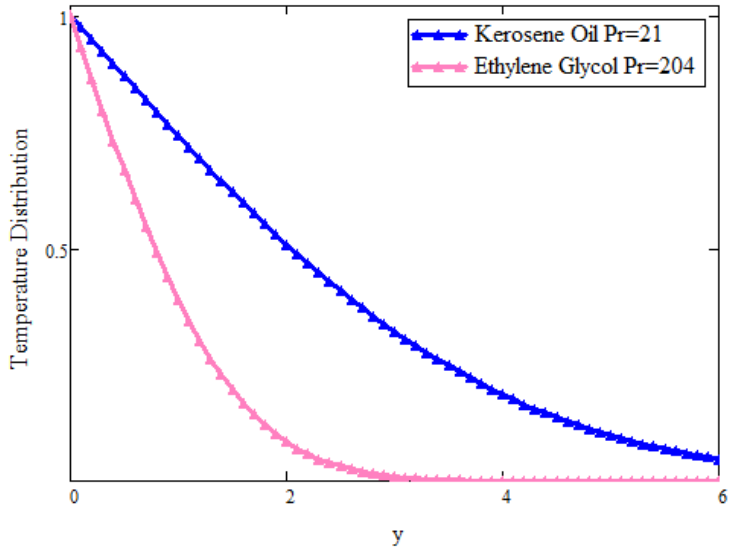

FIGURE 3. The result of Prandtl number (Pr) on temperature Distribution.

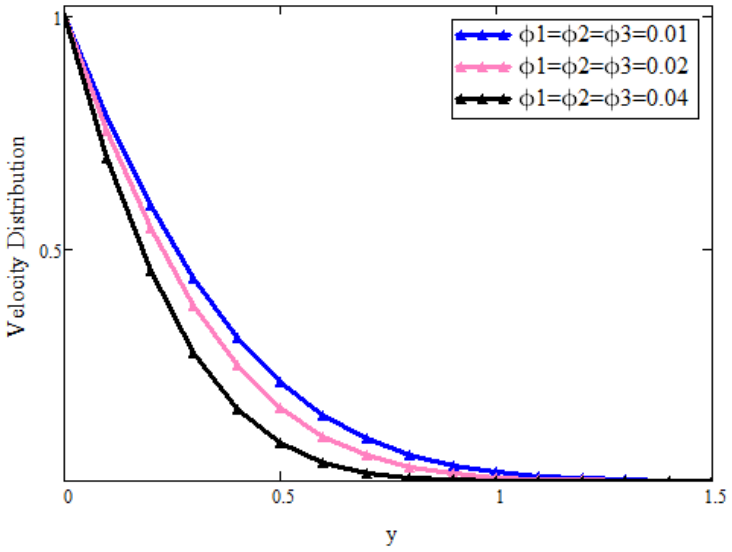

FIGURE 4. The result of velocity distribution on volume fraction parameter of nanofluid ϕ_1,ϕ_2,ϕ_3.

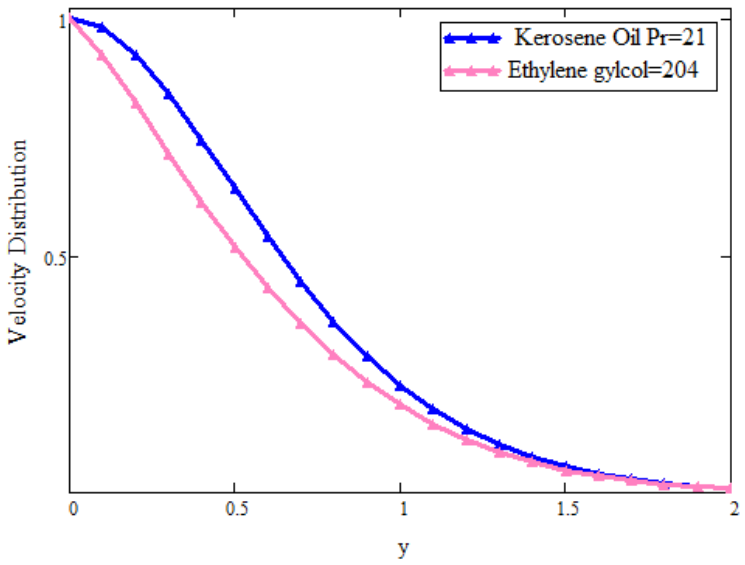

FIGURE 5. The result of Prandtl number (Pr) velocity distribution.

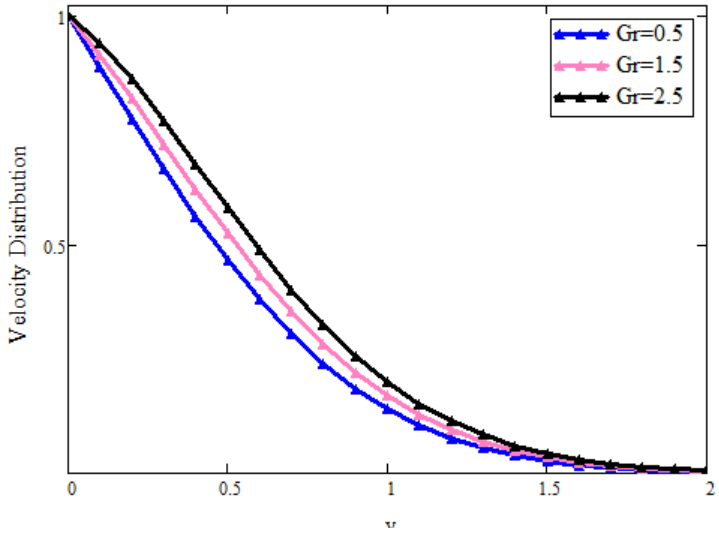

FIGURE 6. The result of Thermal Grashöf number (Pr) on velocity distribution.

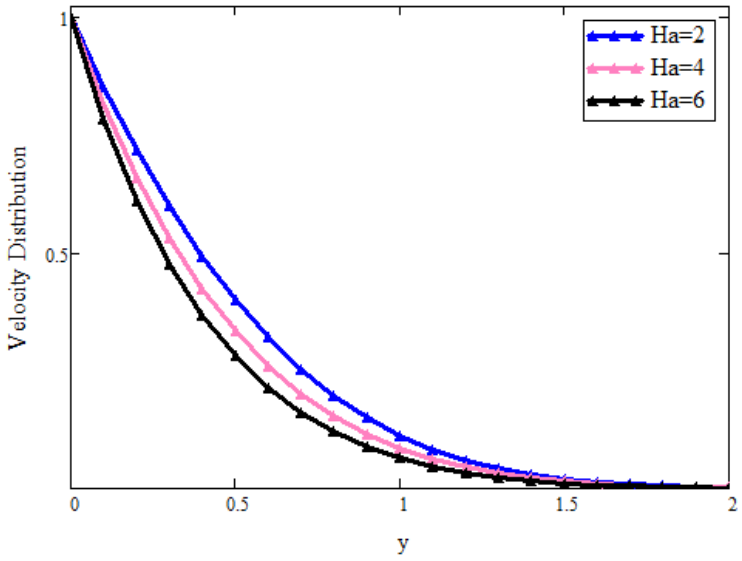

FIGURE 7. The result of magnetic field parameter (Ha) on velocity distribution.

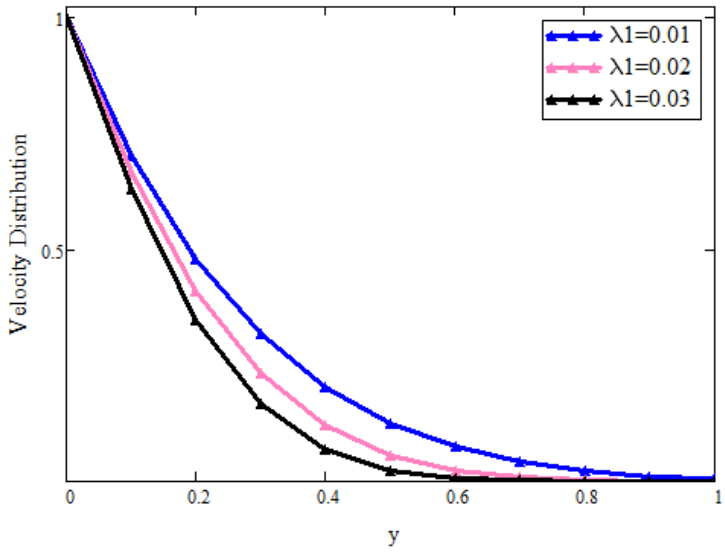

FIGURE 8. The result of time relaxation parameter λ_1 on velocity distribution.

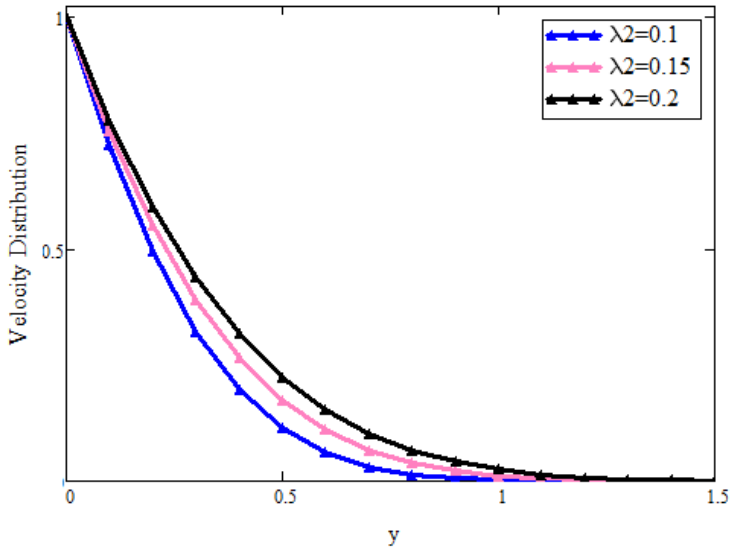

FIGURE 9. The result of time retardation parameter λ_2 on velocity distribution.

NOMENCLATURE

Symbol	Name	Symbol	Name
Q_0	Heat source/sink parameter	Nu	Nusselt number (Dimensionless)
μ	Dynamic viscosity $(kgm^{-1}s^{-1})$	Nr	Radiation parameter
ϕ	Volume fraction parameter of nanofluid	B_0	Utilized magnetic field
v	Velocity field (ms^{-1})	A_1	First Rivilin Erikson tensor
ρ	Density of fluid (kgm^{-3})	J	Current density
T	Cauchy stress tensor	t	Time (s)
ρbg	Body force	I	Identity matrix
A_1	First Rivilin Erikson tensor	Gr	Thermal Grashof number (Dimensionless)
g	Gravitational acceleration	L	Velocity gradient
S_{xy}	Extra stress tensor	β_θ	Coefficient of thermal expansion
σ	Electrical conductivity (s/m)	C_p	Specific heat $(jkg^{-1}K^{-1})$
Pr	Prandtl number (Dimensionless)	k^*	Absorption constant

4. CONCLUSIONS

In this thesis, It has been explored how a fixed oscillating vertical plate behaves as well as a fractional Oldroyd-B nanofluid model. The primary nonlinear system is translated into a dimensionless form using partial differential equations. Laplace transformation is used to find physical reasons for the proposed model. The mean of the graphical facts described in Mathcad are expanded in analytical solutions with parametric effects. The following key

results:

(1) Temperature of fluid can be enhanced by utilizing the larger values of concentration of Ag, Cr and Al_2O_3 nanoparticles while velocity reduced.
(2) This work provides the choice of selection of the suitable base fluids with ternary nanoparticles and found that the temperature and velocity of the fluid achieved maximum values with karocene.
(3) This approach can be utilized to improve the thermophysical properties of the base liquid and applied where needed.
(4) Other parameters have the standard effect on temperature and velocity, which shows the accuracy of the present results with the ternary nanoparticles approach.

Acknowledgments. The authors are thankful to the University of Management and Technology, Lahore, for facilitating this research.

Authors' contributions

Formal analysis, problem formulation M.H.B, M.I.A, M.A.S, and A.H; Investigation, Methodology M.H.B, and M.I.A, Supervision, resources, validation, graphical discussion and software; M.I.A and A.H Review and editing; all authors approved the final version for submission.

Funding

No funding available.

Ethics approval and consent to participate

Not applicable

Consent for publication

Not applicable

Availability of data and material

Data sharing is not applicable to this article as no data sets were generated or analyzed during the current study.

Competing interests

The authors declare that they have no competing interests.

REFERENCES

[1] A. A. Adekunle, S. O. Oparanti, A. Hamzat, and A. A. Abdelmalik. *Dielectric response of vegetable oil-based nanofluid and impregnated Kraft paper for high voltage transformer insulation*. Journal of Molecular Liquids., **39**, no. 1 (2023): 123391.

[2] J. Ahmed, S. Bourazza, M. Sarfraz, M. A. Orsud, S. M. Eldin, N. A. Askar, and M. A. Elkotb. *Heat transfer in Jeffrey fluid flow over a power law lubricated surface inspired by solar radiations and magnetic flux*. Case Studies in Thermal Engineering **49,** no. (2023): 103-220.

[3] A. Ali, M. I. Asjad, M. Usman, and M. Inc. *Numerical solutions of a heat transfer for fractional maxwell fluid flow with water based clay nanoparticles; a finite difference approach*. Fractal and Fractional **5**, no. 4 (2021): 242.

[4] R. Ali, A. Shahzad, K. Saher, Z. Elahi, and T. Abbas. *The thin film flow of Al2O3 nanofluid particle over an unsteady stretching surface*. Case Studies in Thermal Engineering., **29** (2022): 101695.

[5] T. A. Alkanhal, M. Sheikholeslami, M. Usman, R. Haq, A. Shafee, A. S. Ahmadi, and I. Tlili. *Thermal management of MHD nanofluid within the porous medium enclosed in a wavy shaped cavity with square obstacle in the presence of radiation heat source*. International Journal of Heat and Mass Transfer., **139** (2019): 87-94.

[6] S. A. Angayarkanni, V. Sunny, and J. Philip. *Effect of nanoparticle size, morphology and concentration on specific heat capacity and thermal conductivity of nanofluids*. Journal of nanofluids., **4**, no. 3 (2015): 302-309.

[7] T. Anwar, P. Kumam, I. Khan, and W. Watthayu. *Heat transfer enhancement in unsteady MHD natural convective flow of CNTs Oldroyd-B nanofluid under ramped wall velocity and ramped wall temperature*. Entropy., **22**, no. 4 (2020).

[8] T. Anwar, P. Kumam, D. Baleanu, I. Khan, and P. Thounthong. *Radiative heat transfer enhancement in MHD porous channel flow of an Oldroyd-B fluid under generalized boundary conditions*. Physica Scripta., **95**, no. 11 (2020): 115211.

[9] U. Asghar, W. A. Faridi, M. I. Asjad, and S. M. Eldin. *The enhancement of energy-carrying capacity in liquid with gas bubbles, in terms of solitons*. Symmetry **14**, no. 11 (2022): 2294.

[10] U. Asghar, D. Chou, M. I. Asjad, and S. A. O. Abdallah. *Novel soliton solutions of liquid drop model appear in fluid dynamics and modulation instability of dynamical system*. Indian Journal of Physics (2024): 1-14.

[11] P. Cui, Z. Li, Q. Wu, and X. Hou. *Optoelectronic properties and charge transfer dynamics in graphene quantum dot/Ir (III) nanocomposites: Enhancing photocatalytic performance through strategic BTF conjugate binding and end-capping variations*. Diamond and Related Materials **145** (2024): 111107.

[12] S. U. Choi, and J. A. Eastman. *Enhancing thermal conductivity of fluids with nanoparticles.* Argonne National Lab.(ANL), Argonne, (1995): 77.

[13] A. Dawar, N. M. Said, S. Islam, Z. Shah, S. R. Mahmuod, and A. Wakif. *A semi-analytical passive strategy to examine a magnetized heterogeneous mixture having sodium alginate liquid with alumina and copper nanomaterials near a convectively heated surface of a stretching curved geometry*. International Communications in Heat and Mass Transfer **139**, no. 1 (2022): 106452.

[14] Z. Elahi, M. T. Iqbal, and A. Shahzad. *Numerical simulation of heat transfer development of nanofluids in a thin film over a stretching surface*. Brazilian Journal of Physics., **52**, no. 2 (2022): 36.

[15] E. Farooji, E. E. Bajestan, H. Niazmand, and S. Wongwises. *Unconfined laminar nanofluid flow and heat transfer around a square cylinder*. International Journal of Heat and Mass Transfer., **55**, no. 5 (2012): 1475-1485.

[16] M. Fiza, S. Islam, H. Ullah, and Z. Ali. *Mhd thin film oldroyd-b fluid with heat and viscous dissipation over oscillating vertical belts*. Heat Transfer Research., **50**, no. 9 (2019): 145-525.

[17] M. Hamid, M. Usman, T. Zubair, R. U. Haq, and W. Wang. *Shape effects of MoS2 nanoparticles on rotating flow of nanofluid along a stretching surface with variable thermal conductivity: A Galerkin approach*. International Journal of Heat and Mass Transfer **124**, no. 2 (2018): 706-714.

[18] T. Hayat, S. A. Khan, M. I. Khan, S. Momani, and A. Alsaedi. *Cattaneo-Christov (CC) heat flux model for nanomaterial stagnation point flow of Oldroyd-B fluid*. Computer methods and programs in biomedicine., **18**, no. 7 (2020): 105247.

[19] A. Hussain, S. Ghafoor, M. Y. Malik, and S. Jamal. *An exploration of viscosity models in the realm of kinetic theory of liquids originated fluids*. Results in physics **7** (2017): 2352-2360.

[20] M. Javaid, M. Tahir, M. Imran, D. Baleanu, A. Akgül, and M. A. Imran. *Unsteady flow of fractional Burgers' fluid in a rotating annulus region with power law kernel*. Alexandria Engineering Journal., **61**, no. 1 (2022): 17-27.

[21] M. Jawad, K. Shehzad, and R. Safdar. *Novel computational study on MHD flow of nanofluid flow with gyrotactic microorganism due to porous stretching sheet*. Punjab Univ. J. Math., **52**, (2021).

[22] Kazi, M. A., Kharat, V. V., Reshimkar, A. R., and Gophane, M. T. *On Nonlocal Iterative Fractional Terminal Value Problem via Generalized Fractional Derivative*. Punjab Univ. J. Math., **56**, no. 7, 334-347.

[23] A. S. Khan, Y. Nie, and Z. Shah. *Impact of thermal radiation on magnetohydrodynamic unsteady thin film flow of Sisko fluid over a stretching surface*. Processes., **7**, no. 6 (2019): 369.

[24] Q. Li, and Y. Xuan. *Convective heat transfer and flow characteristics of Cu-water nanofluid*. Science in China Series E: Technolgical Science **45** (2002): 408-416.

[25] S. Maripala, and K. Naikoti. *Joule heat parameter effects on unsteady MHD flow over a stretching sheet with viscous dissipation and heat source*. Applications and Applied Mathematics: An International Journal., **14**, no. 4 (2019).

[26] S. Murad, M. Amin, and F. K. Hamasalh. *Numerical study for fractional-order magnetohydrodynamic boundary layer fluid flow over stretching sheet*. Punjab Univ. J. Math., **55**, 2 (2023).

[27] A. S. Oke. *Heat and mass transfer in 3D MHD flow of EG-based ternary hybrid nanofluid over a rotating surface*. Arabian Journal for Science and Engineering., **47**, no. 12 (2022): 16015-16031.

[28] R. Prasher, D. Song, J. Wang, and P. Phelan. *Measurements of nanofluid viscosity and its implications for thermal applications*. Applied physics letters **89**, 13 (2006).

[29] M. Qasim, and O. D. Makinde. *Entropy Generation Due to Heat and Mass Transfer in a Flow of Dissipative Elastic Fluid Through a Porous Medium*. **29**, 10 (2017).

[30] M. Ramezanizadeh, M. A. Nazari, M. H. Ahmadi, and E. Açıkkalp. *Application of nanofluids in thermosyphons: a review*. Journal of Molecular Liquids., **27**, no. 2 (2018): 395-402.

[31] M. Ramzan, F. Ali, N. Akkurt, A. Saeed, P. Kumam, and A. M. Galal. *Computational assesment of Carreau ternary hybrid nanofluid influenced by MHD flow for entropy generation*. Journal of Magnetism and Magnetic Materials **567** (2023): 170353.

[32] M. B. Riaz, A. U. Rehman, A. Wojciechowski, and A. Atangana. *Heat and mass flux analysis of magneto-free-convection flow of Oldroyd-B fluid through porous layeblack inclined plate*. Scientific Reports **13**, 1 (2023): 653.

[33] B. L. Rios, M. S. Carlos, I. R. Solorio, and K. D. P. Nigam. *An overview of sustainability of heat exchangers and solar thermal applications with nanofluids: A review*. Renewable and Sustainable Energy Reviews **14**, 2 (2021): 110855.

[34] R. R. Sahoo, and V. Kumar. *Development of a new correlation to determine the viscosity of ternary hybrid nanofluid*. International Communications in Heat and Mass Transfer **111** (2020): 104451.

[35] N. A. Shah, A. Wakif, E. R. E. Zahar, T. Thumma, and S. J. Yook. *Heat transfers thermodynamic activity of a second-grade ternary nanofluid flow over a vertical plate with Atangana-Baleanu time-fractional integral*. Alexandria Engineering Journal., **61**, no. 12 (2022): 10045-10053.

[36] A. Shahzad, F. Liaqat, Z. Ellahi, M. Sohail, M. Ayub, and M. R. Ali. *Thin film flow and heat transfer of Cu-nanofluids with slip and convective boundary condition over a stretching sheet*. Scientific Reports., **12**, no. 1 (2022): 14254.

[37] M. Sheikholeslami, D. D. Ganji, and M. M. Rashidi. *Magnetic field effect on unsteady nanofluid flow and heat transfer using Buongiorno model*. Journal of Magnetism and Magnetic Materials **416** (2016): 164-173.

[38] Y. Q. Song, A. Farooq, M. Kamran, S. Rehman, M. Tamoor, R. Khan, A. Fahad, and M. I. Qureshi. *Analytical Solution of Fractional Oldroyd-B Fluid via Fluctuating Duct*. Complexity., **21**, no. 1 (2021): 9576873.

[39] A. B. Suleimanov, F. S. Ismailov, and E. F. Veliyev. *Nanofluid for enhanced oil recovery*. Journal of Petroleum science and Engineering **78**, 2 (2011): 431-437.

[40] A. Tassaddiq. *MHD flow of a fractional second grade fluid over an inclined heated plate*. Chaos, Solitons and Fractals **123** (2019): 341-346.

[41] B. Thomases, and M. Shelley. *Emergence of singular structures in Oldroyd-B fluids*. Physics of fluids., **19**, (2007).

[42] M. T. Usman, M. Zubair, Hamid, and R. U. Haq. *Novel modification in wavelets method to analyze unsteady flow of nanofluid between two infinitely parallel plates*. Chinese Journal of Physics **66** (2020): 222-236.

[43] F. Wang, S. Rehman, J. Bouslimi, H. Khaliq, M. I. Qureshi, M. Kamran, A. N. Alharbi, H. Ahmad, and A. Farooq. *Comparative study of heat and mass transfer of generalized MHD Oldroyd-B bio-nano fluid in a permeable medium with ramped conditions*. Scientific reports., **11**, no. 1 (2021): 2345

[44] J. Wang, M. I. Khan, W. A. Khan, and S. Z. Abbas. *Transportation of heat generation/absorption and radiative heat flux in homogeneous–heterogeneous catalytic reactions of non-Newtonian fluid (Oldroyd-B model)*. Computer Methods and Programs in Biomedicine **189** (2020): 1053.

[45] T. A. Yusuf, F. Mabood, W. Ali Khan, and J. A. Gbadeyan. *Irreversibility analysis of Cu-TiO2-H2O hybrid-nanofluid impinging on a 3-D stretching sheet in a porous medium with nonlinear radiation: Darcy-Forchheimer's model*. Alexandria Engineering Journal., **59**, no. 6 (2020): 5247-5261.

[46] M. Zhang, I. Lashgari, T. A. Zaki, and L. Brandt. *inear stability analysis of channel flow of viscoelastic Oldroyd-B and FENE-P fluids*. Journal of fluid mechanics **737** (2013): 249-279.